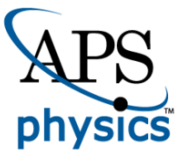

Electrokinetic instability in microchannels

Jarrod Schiffbauer, Evgeny A. Demekhin, and Georgy Ganchenko

Phys. Rev. E **85**, 055302 — Published 18 May 2012

DOI: 10.1103/PhysRevE.85.055302

Electrokinetic Instability in Micro-channels

Jarrod Schiffbauer,[1] Evgeny A. Demekhin,[2] and Georgy Ganchenko[2]

[1] *Faculty of Mechanical Engineering, Micro- and Nanofluidics Laboratory, Technion - Israel Institute of Technology - Technion City 32000, Israel*

[2] *Dept. of Computation Mathematics and Computer Science Kuban State University Krasnodar, 350040, Russian Federation.*

(Dated: April 27, 2012)

The effect of geometric confinement on electro-convective instability due to non-equilibrium electro-osmotic slip at the interface of an electrolytic fluid and charge-selective solid is studied. It is shown that the topology of the marginal stability curves and the behavior of the critical parameters depend strongly on both channel geometry and dimensionless Debye length at low voltages for sufficiently deep channels, corresponding to the Rubsinstein-Zaltzman instability mechanism, but that stability is governed almost entirely by channel depth for narrow channels at higher voltages. For shallow channels, it is shown that above a transition threshold, determined by both channel depth and Debye length, the low-voltage instability is completely suppressed.

PACS numbers: 47.61.Fg, 47.57.jd, 47.20.Ma,82.39.Wj

I. INTRODUCTION

Electro-convective (Rubinstein-Zaltzman) instability and its relationship to the overlimiting conductance of charge-selective interfaces has garnered significant attention in recent years (see [1]–[9]). Not only is it of practical significance for applications as diverse as desalination, fuel cells, and microfluidic analysis systems, but the strong coupling between electro-diffusion and hydrodynamics leads to very rich spatio-temporal behavior. Specifically, as the current density through the charge-selective solid exceeds the classical limiting value, the depleted region of the concentration polarization layer structure can no longer maintain local electro-neutrality and an extended space-charge (ESC) region develops between the regular quasi-equilibrium electric double-layer and the electro-neutral diffusion layer [1]; the latter extending either to bulk, or to an electrode, depending on the size of the system relative to the interval of observation. Due to the non-monotonic nature of charge density – hence gradient in the electric body force– in the ESC, the system loses mechanical stability in a way reminiscent of Benard or Marangoni convection. This instability can lead to the formation of vortex arrays which limit the extent of the depleted diffusion boundary layer adjacent to a charge-selective interface, thus in turn leading to an increase in electric current owing to an effectively decreased resistance of the depleted region. Much of the foundational theoretical work concerns open systems, i.e. relatively large electrolytic cells bounded by planar membranes or electrodes which may be considered infinite in the transverse directions; thus, in the absence of geometric inhomogeneity and prior to the threshold of instability, the fundamental problem is effectively one-dimensional (1D). Such a description captures these effects well in systems with dimensions on the order of cm^2 or mm^2, predicting a voltage threshold for instability around a volt or slightly less,

which has been confirmed experimentally (see [10]– [12]). However, a number of experimental observations of related effects in systems confined to microchannels exhibit thresholds on the order of 10's of volts and higher ([12],[13]–[16].) Furthermore, recent experimental ([5]) and numerical ([6]) studies show that microchannel geometry can impact the overlimiting conductance and for sufficiently small microchannels and effectively suppress the instability at voltages as high as 40V. This study serves to provide a theoretical framework to bridge this gap, and in the process of doing so, also predicts novel effects due to a competition between stabilizing and de-stabilizing effects reminiscent of Taylor-Couette instabilities ([7, 8]). It is worth noting that previous work has been done regarding the effects of confinement on vortical convection in Hele-Shaw geometries [17, 18]. Regarding electro-convective instability, relatively wide boundaries in the x-direction have been shown to result in a wavelength selection process which ultimately chooses maximum vortex size essentially corresponding to the allowed standing perturbation modes in this direction [1, 9]. However, this represents, to our knowledge, the first study of the specific effects of narrow confinement in the z-direction on electroconvective instability.

II. FORMULATION AND ASSUMPTIONS

We consider a symmetric, binary electrolyte with a diffusivity of cations and anions $\tilde{D}$, dynamic viscosity $\tilde{\mu}$ and permittivity $\tilde{d}$, confined to a microchannel with insulating walls at $\tilde{z} = \pm\tilde{h}$ and bounded by an ideal, semi-selective ion-exchange membrane surface, $\tilde{y} = 0$ and by an outer edge of the diffusion layer, $\tilde{y} = \tilde{\delta}$ with the bulk concentration $\tilde{c}_0$. Notations with tilde are used for the dimensional variables, as opposed to their dimensionless counterparts without. $\{\tilde{x},\ \tilde{y},\ \tilde{z}\}$ are the coordinates, where $\tilde{x}$ is directed along the membrane surface, $\tilde{y}$ is normal to the membrane surface, $\tilde{z}$ is normal to the micro-channel plane. The flow is assumed to be Hele-Shaw, with non-conductive walls $\tilde{z} = \pm\tilde{h}$, impermeable to both kinds of ions. No-slip conditions on the walls and at the membrane surface are assumed. The potential $\tilde{\Phi}$ and concentrations $\tilde{c}^{\pm}$ are assumed constant in the $\tilde{z}$-direction, while velocity components $\tilde{u}$ and $\tilde{v}$ have a parabolic Poiseuille distribution with respect to $\tilde{z}$, $\tilde{u} = \frac{3}{2}\tilde{U}(1 - \tilde{z}^2/\tilde{h}^2)$ and $\tilde{v} = \frac{3}{2}\tilde{V}(1 - \tilde{z}^2/\tilde{h}^2)$, and the third velocity component is zero, $\tilde{w} = 0$, so the averaged velocity vector $\mathbf{U} = U\hat{i} + V\hat{j}$. Then the system of equations averaged with respect to the channel width is as follows,

$$\frac{\partial c^+}{\partial t} + U\frac{\partial c^+}{\partial x} + V\frac{\partial c^+}{\partial y} = \frac{\partial}{\partial x}(c^+\frac{\partial \Phi}{\partial x}) + \frac{\partial}{\partial y}(c^+\frac{\partial \Phi}{\partial y}) + \frac{\partial^2 c^+}{\partial x^2} + \frac{\partial^2 c^+}{\partial y^2} \tag{1}$$

$$\frac{\partial c^-}{\partial t} + U\frac{\partial c^-}{\partial x} + V\frac{\partial c^-}{\partial y} = -\frac{\partial}{\partial x}(c^-\frac{\partial \Phi}{\partial x}) - \frac{\partial}{\partial y}(c^-\frac{\partial \Phi}{\partial y}) + \frac{\partial^2 c^-}{\partial x^2} + \frac{\partial^2 c^-}{\partial y^2} \tag{2}$$

$$\varepsilon^2\left(\frac{\partial^2 \Phi}{\partial x^2} + \frac{\partial^2 \Phi}{\partial y^2}\right) = c^- - c^+, \tag{3}$$

$$\frac{\partial P}{\partial x} = \frac{\partial^2 U}{\partial x^2} + \frac{\partial^2 U}{\partial y^2} - \frac{3}{h^2}U - \frac{\kappa}{\varepsilon^2}(c^+ - c^-)\frac{\partial \Phi}{\partial x}, \tag{4}$$

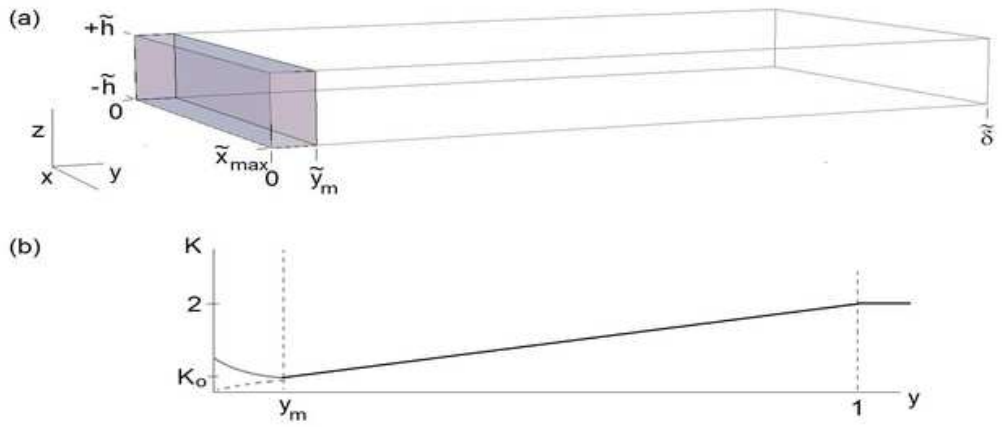

Figure 1: Depictions of (a) the model geometry and coordinate system (dimensional coordinates), and (b) the quasi-1D concentration profile (dimensionless coordinates.) In (a) the space charge region containing both a macroscopic extended space-charge (ESC) and microscopic electric double layer (EDL) are shown shaded with the outer boundary at the plane $y = y_m$. This corresponding region in (b) shows a qualitative sketch of the cation (solid gray) and anion (dashed gray) concentrations. The diffusion layer electro-neutral concentration is approximately linear and shown in black.

$$\frac{\partial P}{\partial y} = \frac{\partial^2 V}{\partial x^2} + \frac{\partial^2 V}{\partial y^2} - \frac{3}{h^2} V - \frac{\kappa}{\varepsilon^2}(c^+ - c^-)\frac{\partial \Phi}{\partial y}, \tag{5}$$

$$\frac{\partial U}{\partial x} + \frac{\partial V}{\partial y} = 0, \tag{6}$$

The system is taken in a dimensionless form with $\tilde{\delta}$ as a characteristic length, $\tilde{\delta}^2/\tilde{D}$ as a characteristic time, $\tilde{\mu}$ as a dynamical characteristic value, thermodynamic potential $\tilde{\Phi}_0 = \tilde{R}\tilde{T}/\tilde{F}$ is taken as a characteristic potential and the bulk concentration $\tilde{c}_0$ as a characteristic concentration. The parameter $\kappa = \tilde{d}\tilde{\Phi}_0/\tilde{\mu}\tilde{D}$, appears as a coupling coefficient between hydrodynamics and electrostatics. It is essentially an electrokinetic Peclet number depending upon the properties of the electrolyte and not upon the properties of an imposed flow. Here velocity components U and V are averaged with respect to z, P is the averaged pressure and ε is the dimensionless Debye length, $\varepsilon = \tilde{\lambda}_D/\tilde{\delta}$ and $\tilde{\lambda}_D = \sqrt{\tilde{d}\tilde{\Phi}_0/\tilde{F}\tilde{c}_0}$, $\tilde{R}$ is the universal gas constant, $\tilde{T}$ is the absolute temperature, and $\tilde{F}$ is the Faraday constant.

The important $O(1/h^2)$ terms at $h \to 0$ originate from the wall friction. Keeping in (4)-(5) only leading order terms in h leads to the Darcy's law

$$\mathbf{U} = -\frac{h^2}{3}\nabla P - \frac{\kappa h^2}{3\varepsilon^2}\rho\nabla\Phi,$$

corrected by the Coulomb force, where $\rho = c^+ - c^-$ is the space charge density. However, we shall keep in (4)-(5) all order terms to satisfy the boundary conditions on the membrane surface, $y = 0$.

Our choice of boundary conditions at the planes $y = 0, 1$ is consistent with a simplified model of the concentration polarization layer (CPL) structure on the anodic (depleted) side of a highly charge-selective element such as a porous membrane or nanoslot – represented here by a perfectly selective membrane with a fixed,

uniform cation concentration and complete anion exclusion– and bounded by a stirred bulk at $y = 1$ (see Fig. 1.)

The boundary conditions at the membrane surface are as follows,

$$y = 0: \qquad c^+ = p, \quad -c^- \frac{\partial \Phi}{\partial y} + \frac{\partial c^-}{\partial y} = 0, \qquad U = V = 0, \qquad \Phi = 0. \tag{7}$$

The first condition, prescribing interface concentration equal to that of the fixed charges inside the membrane, is asymptotically valid for large p and is first introduced by Rubinstein (see, for example, [3] and corresponding references) to avoid solution inside the membrane. The second condition means that the membrane is an ideally permselective one and, hence, there is no-flux for anions. The third condition is usual no-slip condition and the last condition fixes zero potential the membrane surface.

The boundary conditions at the outer edge of the diffusion layer specify both concentrations, vanishing of the velocity component V and shear stress and ΔV specifies a drop of potential across the diffusion layer [1]-[2],

$$y = 1: \qquad c^+ = 1, \quad c^- = 1, \qquad V = 0, \quad \frac{\partial U}{\partial y} + \frac{\partial V}{\partial x} = 0, \qquad \Phi = \Delta V. \tag{8}$$

The problem is described by four dimensionless parameters: ΔV, ε, κ and $h = \tilde{h}/\tilde{\delta}$. Dependence on the concentration p for the over-limiting regimes is practically absent and, hence, p is not included in the mentioned parameters. For systems confined to a small channel, in addition to the usual small parameter ε, (1)–(8), the system also has a second small parameter, h.

III. ASYMPTOTICAL SOLUTION

Non-equilibrium slip velocity in a micro-channel. For $\varepsilon \to 0$ and current densities above the limiting value, the interval $0 < y < 1$ is divided into two regions: (a) a space-charge region, $0 < y < y_m$ and (b) electro-neutral region, $y_m < y < 1$. The problem (1)-(8) has a 1D steady solution, which coincides with the classical statement for perfect semi-selective membrane [1]– [2] and it has a well-known solution for the potential in the space charge region

$$\Phi = \Delta V \left[1 - (1 - \frac{y}{y_m})^{3/2} \right], \tag{9}$$

where the potential drop in ESC is given by the following expression,

$$\frac{2\sqrt{2j}}{3\varepsilon} y_m^{3/2} = \Delta V. \tag{10}$$

If uniformity in x direction is violated, the velocity field will be perturbed from zero. Following [2] and solving (4)–(6), taking into account $1/h$-terms, inside ESC region yields the slip velocity at the boundary y_m

$$U_m = -\frac{\kappa}{8} \Delta V^2 \frac{1}{j} \frac{\partial j}{\partial x} \cdot f(\frac{y_m}{h}) \tag{11}$$

with the correction term for a micro-channel,

$$f(\frac{y_m}{h}) = 2\frac{h^2}{y_m^2} \left[\frac{1}{\sqrt{3}} \frac{h}{y_m} \tanh \frac{y_m \sqrt{3}}{h} - \frac{1}{\cosh \frac{y_m \sqrt{3}}{h}} \right].$$

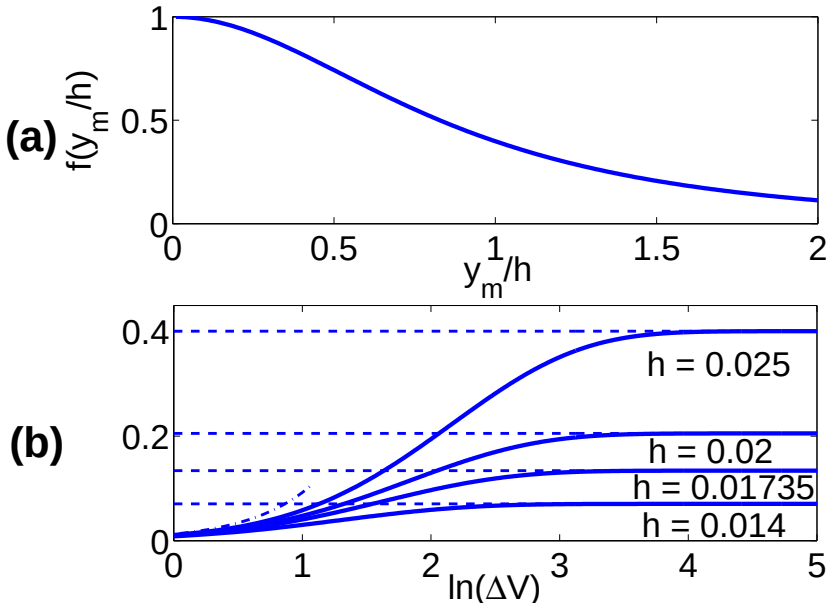

Figure 2: (a)Function of the confinement influence, $f(y_m/h)$. Note that for sufficiently small values of y_m/h, $f \to 1$ and the slip velocity approaches the un-confined (Rubinstein-Zaltzman) case. (b) Slip velocity U_m as a function of ΔV at unit $\partial j/\partial x$ and parameterized with h at $\varepsilon = 10^{-4}$; dashed-dotted line stands for the un-confined limit.

Here $y_m = 9^{1/3}\varepsilon^{2/3}\Delta V^{2/3}/2j^{1/3}$ is found from (10).

(a) If $y_m/h \to 0$, i.e. for very wide (essentially unconfined) channels, $f \to 1$ and the famous Rubinstein slip velocity for the phenomena of the second kind is obtained.

(b) If $\Delta V \to \infty$, $y_m/h \to \infty$ and $f(y_m/h) \to 0$ and two factors in (11) cancel each other and it turns into

$$U_m = -\frac{2\kappa}{9\sqrt{3}} \cdot \frac{h^3}{\varepsilon^2} \cdot \frac{\partial j}{\partial x}. \tag{12}$$

Solution in the electro-neutral region. Stability analysis. Introduction of the stream-function Ψ from the expressions $U = \partial\Psi/\partial y$ and $V = -\partial\Psi/\partial x$ along with well-known algebraic calculations turn the system (4)–(6) to the single fourth-order partial differential equation for the stream-function. In the electroneutral region $c^+ = c^-$ and this equation is,

$$\frac{\partial^4\Psi}{\partial x^4} + 2\frac{\partial^4\Psi}{\partial x^2\partial^2 y} + \frac{\partial^4\Psi}{\partial y^4} - \frac{3}{h^2}\left(\frac{\partial^2\Psi}{\partial x^2} + \frac{\partial^2\Psi}{\partial y^2}\right) = 0 \tag{13}$$

with the boundary conditions

$$y = y_m : \Psi = 0, \qquad \frac{\partial\Psi}{\partial y} = U_m, \quad y = 1 : \quad \Psi = 0, \qquad \frac{\partial^2\Psi}{\partial y^2} = 0. \tag{14}$$

Note the fourth term, equal to $3/h^2$ times the vorticity, where $h \to 0$ is a small parameter. This corresponds to viscous shearing interaction between the fluid and the channel walls and gives rise to stability characteristics quite different than the unconfined membrane case. Far from the boundary y_m terms $\nabla^4\Psi$ can be dropped, but these terms become important to satisfy the boundary conditions at $y = y_m$. Because of this fact there is a thin

boundary layer $O(h)$ near $y = y_m$ and there is a possibility to build up asymptotic outer and inner expansions with their following matching. However, we prefer to keep in (13) all order terms.

For the salt concentration $K = c^+ + c^-$ we have the following equations,

$$\frac{\partial K}{\partial t} + U\frac{\partial K}{\partial x} + V\frac{\partial K}{\partial y} = \frac{\partial^2 K}{\partial x^2} + \frac{\partial^2 K}{\partial y^2} \tag{15}$$

Then, treating the edge of the space charge region as the boundary,

$$y = y_m : \quad K = a\Big(\varepsilon\frac{\partial K}{\partial y}\Big)^{2/3}, \quad y = 1 : \quad K = 2. \tag{16}$$

The first boundary condition is worth some discussion. In the space charge region, which is also called a depletion region, the salt concentration K is small, $K = O(\varepsilon^{2/3})$. Outside of this region $K = O(1)$. The attempts in [1] to solve (15) with the boundary condition at $y = y_m$ taken in the first approximation, $K = 0$, led to a singularity. Physically this singularity originates from an infinite electric resistance at $K = 0$. In order to treat this singularity, higher order terms, $O(\varepsilon^{2/3})$, must be included in the analysis. Such treatment was done in [2] and the details were presented in [3]. We refer a reader to a sophisticated analysis of this work. Here we employ the boundary condition of [2], Eqn. (4). The approach reduces Eqs. (1)-(3) to a single (Painleve) differential equation for the electric field, and the constant, $a \approx 0.9666$, is obtained numerically.(see [3]).

The unperturbed solution is given by

$$K_0 = j(y - y_m) + a(\varepsilon j)^{2/3}, \qquad y_m = 1 - \frac{2}{j} + a\varepsilon^{2/3} j^{-1/3}.$$

At sufficiently large potential drop ΔV the 1D solution succumbs to the electroconvective instability. In contrast to the classical un-confined Rubinstein-Zaltzman instability, the viscous damping is expected to reduce this instability and become more efficient for smaller thickness h. Note that electroconvective motion in the presence of z-confinement was predicted and observed in the context of electrodeposition where it was also noted that this tended to suppress gravitational convection (see [17],[18].) However, the cells were not sufficiently shallow (h on the order of mm) to have much of an effect on electroconvection in these cases.

To ascertain the threshold voltage for the onset of the vortex instability, the stability analysis is restricted by seeking the conditions for which the exponential decay is changed to the exponential growth, i.e. only those modes at a given voltage for which the exponential growth rate of the disturbance is zero, otherwise known as 'marginally stable.' Therefore, assuming small neutral (time-independent) sinusoidal perturbations about this solution,

$$K = K_0(y) + \hat{K}(y)\exp(i\alpha x), \quad \Psi = \hat{\Psi}(y)\exp(i\alpha x), \quad U_m = \hat{U}_m\exp(i\alpha x) \tag{17}$$

and linearizing (13) - (16) with respect to the perturbations turns the system into a linear ODE system,

$$\Psi^{\hat{I}V} - 2\alpha^2\hat{\Psi}'' + \alpha^4\hat{\Psi} - \frac{3}{h^2}\left(\hat{\Psi}'' - \alpha^2\hat{\Psi}\right) = 0, \tag{18}$$

$$y = y_m : \quad \hat{\Psi} = 0, \quad \hat{\Psi}' = \hat{U}_m, \quad y = 1 : \quad \hat{\Psi} = 0, \quad \hat{\Psi}'' = 0, \tag{19}$$

$$\hat{K}'' - \alpha^2\hat{K} = -i\alpha K'\hat{\Psi}, \tag{20}$$

$$y = y_m : \quad \hat{K} = \frac{\varepsilon^{2/3}}{3}\left\{\frac{2a}{j^{1/3}} + \frac{2^{1/3}}{j^{1/3}}\cdot\left(\frac{3}{4}\Delta V\right)^{2/3}\right\}\cdot\hat{K}'(0), \quad y = 1 : \quad \hat{K} = 0. \tag{21}$$

Here

$$\hat{U}_m = \hat{\Psi}' = -\frac{\kappa}{8}\frac{\Delta V^2}{j}\cdot i\alpha\hat{K}'(0)\cdot f(\frac{y_m}{h}), \quad y_m = \frac{3\varepsilon^{2/3}}{2\cdot 3^{1/3}j^{1/3}}\Delta V^{2/3} \tag{22}$$

Solution of (18)–(22) gives the dispersion relation for the marginal stability curves:

$$\frac{\kappa}{8}\cdot\Delta V^2\cdot f\left(\frac{y_m}{h}\right) = -\frac{6\sinh^2\alpha\left[\coth\alpha - \dfrac{\sigma}{\alpha}\coth\sigma\right](1+\alpha\,\coth\alpha\cdot N)}{h^2\,\sinh^2\alpha\,[(\sigma^2+\alpha^2)\,\coth\alpha - 2\,\alpha\,\sigma\,\coth\sigma] - 3\,\alpha}, \tag{23}$$

with

$$N \equiv \frac{\varepsilon^{2/3}}{3}\left\{\frac{2a}{j^{1/3}} + \frac{2^{1/3}}{j^{1/3}}\cdot\left(\frac{3}{4}\Delta V\right)^{2/3}\right\}, \quad \sigma \equiv \frac{\sqrt{3}}{h}\left(1+\frac{\alpha^2h^2}{3}\right)^{1/2}.$$

For $h\to\infty$ we approach the usual membrane case, $\sigma\to\alpha$, $f(y_m/h)\to 1$ and (23) turns into

$$\frac{\kappa}{8}\cdot\Delta V^2 = 4\frac{\sinh\alpha\cosh\alpha - \alpha + N\alpha(\cosh^2\alpha - \alpha\coth\alpha)}{\sinh\alpha\cosh\alpha + \alpha - 2\alpha^2\coth\alpha} \tag{24}$$

which coincides with the expression (33) from [2] and for $\varepsilon = 0$ with the expression (94) of [1].

IV. RESULTS AND DISCUSSION

The marginal stability curves are obtained by solution of the dispersion relation (23); results are presented in Fig. 3. For sufficiently deep micro-channels, the curves approach the unconfined membrane case. This is also evident from the asymptotic expression (24) which is equivalent to the unconfined membrane case for $f\to 1$. As the micro-channel depth is decreased, new behaviors become evident. As the channel depth decreases, the critical voltage rises and the region of instability becomes narrower, eventually becoming pinched on either side of the critical wavenumber. At a channel depth of approximately $h = h_* \approx 0.01735$, the marginal stability curve undergoes a change in topology and the pinch develops into a closed island of instability at lower critical voltages corresponding to the primary Rubinstein-Zaltzman instability with a secondary (open) instability at higher voltages. The separatrix is shown in the figure by the dashed line.

This behavior is seen in a variety of systems wherein there is a competition between multiple instability mechanisms, such as the aforementioned Taylor-Couette flow (see [7] and references therein.) In the context of the present system, the physical explanation is as follows: At low vorticity, corresponding to low local fluid velocity near and slightly above the lowest critical voltage, viscous shearing between the flow and the walls at $z = \pm h$ represented by the $O(h^{-2})$ term in Eqn. 13 tends to stabilize the flow via dissipation, as one would intuitively expect. For sufficiently narrow channels, this leads to the appearance of a maximally unstable critical voltage, i.e. the "top" of the island where the stabilizing effects of viscous shear begin to exceed the de-stabilizing effects of the forces in the extended space charge region, represented here by the modified slip

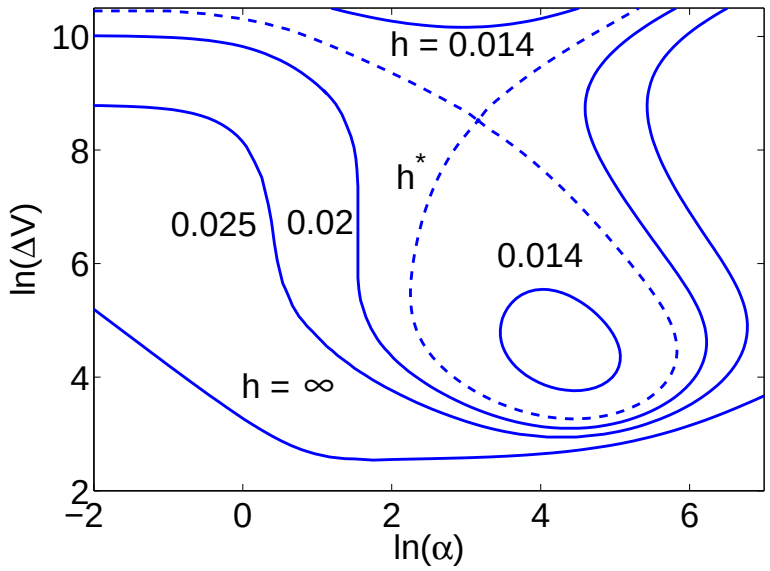

Figure 3: Topology of marginal stability curves for $\kappa = 0.2$ and $\varepsilon = 10^{-4}$ and for different values of the parameter h. The separatrix takes place at $h = h^* \approx 0.01735$.

velocity. However, at higher vorticity, corresponding to higher local velocity at yet higher voltages, viscous diffusion of momentum will tend to de-stabilize the flow, leading to the secondary shear instability and secondary critical voltage minimum above the island. Such a dual role for viscosity is discussed in the context of Taylor-Couette flow in [8] and in the context of shearing instability in thin channels in [19].

The critical parameters of threshold of instability, α_* and ΔV_* giving the critical mode and the corresponding critical voltage for this mode, are determined by the condition $\partial \Delta V / \partial \alpha|_{\alpha=\alpha_*} = 0$. Plots of the critical parameters vs. inverse channel depth for several values of dimensionless Debye length help to clarify the nature of these changes (see Figs. 4 (a) and (b).) Three regimes may be identified from these results. For sufficiently deep channels, (23), in fact, coincides with (24), corresponding to the usual instability of the extended space charge, and is strongly governed by the slip velocity with $f = 1$ in (11). The system has one critical point. For sufficiently narrow channels and high voltages the system is governed by the slip velocity (12) and the system is essentially independent of concentration and governed entirely by channel geometry. The system again has a single critical point. A transitional region may be identified, which depends strongly on the Debye parameter, wherein the solution topology changes, corresponding to the island of instability in Fig. 3. Such topology of the critical parameters gives rise to a hysteresis: with reference to Fig. 4 part (a), if we were to gradually decrease the channel depth, the system would eventually jump to the lower branch of the critical curve (the jump shown by the dashed line.) The jump from the lower branch to the upper on takes place in another point, for the larger confinement depth h. However, it should be noted that under typical experimental conditions, the voltage for these secondary instabilities can be quite high, corresponding to (dimensional) applied voltages greater than 1

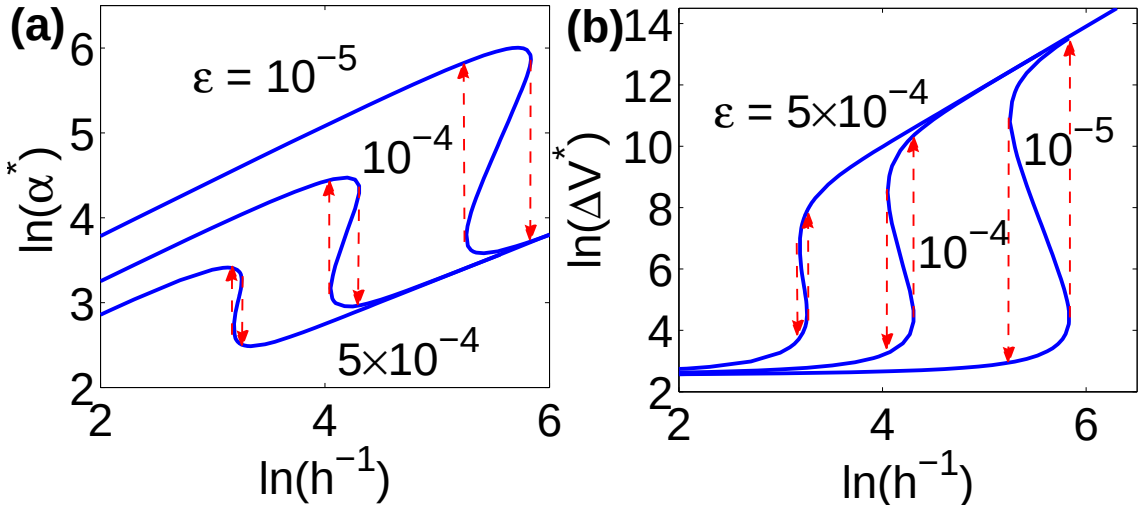

Figure 4: Critical wavenumber (a) and critical voltage vs. inverse channel depth for $\kappa = 0.2$ and different ε.)

kV.

The general trend that decreasing micro-channel depth increases the critical voltage for onset of instability is qualitatively consistent with the observations of Yossifon et. al.[5] The increase in critical wavenumber with decreasing channel depth is consistent with the intuitive idea that the most unstable perturbations should scale with the channel dimension. The existence of a secondary instability at high voltages is also consistent with analysis of experimental data in which the primary instability vortices are observed to disappear and preliminary evidence suggests transient vortices occur at a later time [14].

E.D. and G.G. were supported in part by Russian Foundation for Basic Research (projects no. 11-08-00480-a and no. 11-01-96505-r_yug_ts). J.S. was supported by NASA WV Space Grant Consortium (Grant NNX10AK62H.) E.D. also acknowledges National Science Foundation support through CBET-1066730. This work originated in the visit to MIT hosted by M. Bazant, when this problem was suggested to E.D.

[1] I. Rubinstein and B. Zaltzman , Physical Review E. **62**, 2238 (2000).

[2] I. Rubinstein and B. Zaltzman , Physical Review E. **68**, 032501 (2003).

[3] B. Zaltzman and I. Rubinstein, J. Fluid Mech. **579**, 173 (2007).

[4] G. Yossifon and H.-C. Chang, PRL, **101**, 254501 (2008).

[5] G. Yossifon and P. Mushenheim and H.-C. Chang, EPL, **90**, 64004 (2010).

[6] E. V. Dydek and B. Zaltzman and I. Rubinstein and D. S. Deng and A. Mani and M.Z. Bazant, Phys. Rev. Lett. **107**, 118301(2011).

[7] A. Meseguer and F. Marques, J. Fluid Mech., **402**, 33 (2000).

[8] C.-Y. Yih, Phys. Fluids, **4**,806 (1961).

[9] E. Demekhin, V. Shelistov and S. Polyanskikh, Physical Reveiw E. **84**, 036318 (2011).

[10] S. J. Kim ,Y.-C. Wang , J. H. Lee ,H. Jang, J. Han, Phys. Rev. Lett. **99**, 044501.1.(2007).

[11] S. M. Rubinstein, G. Manukyan ,A. Staicu , I. Rubinstein, B. Zaltzman , R. G. H. Lammertink,F. Mugele ,M. Wessling, Phys. Rev. Lett. **101**, 236101 (2008).

[12] G. Yossifon,H.-C. Chang Phys. Rev. Lett. **101**. 254501 (2008).

[13] J. Schiffbauer,. W. Booth, K. Kelley, B. Edwards, and A. Timperman "Current rectifcation at a charge-selective element due to asymmetric concentration polarization,," Manuscript in submission.

[14] J. Schiffbauer, Doctoral dissertation (2011).

[15] G. Yossifon, P. Mushenheim, Y.-C. Chang, and H.-C. Chang, Phys. Rev. E. **81**, 046301 (2010).

[16] G. Yossifon, Y.-C. Chang, and H.-C. Chang, Phys. Rev. Lett. **103**, 154502 (2009).

[17] V. Fleury J.-N. Chazalviel, and M. Rosso, Phys. Rev. Lett. **68**, 2492 (1992).

[18] J.M. Huth, H.L. Swinny, W.D. McCormick, A. Kuhn, and F. Argoul, Physical Reveiw E. **51**, 3444 (1995).

[19] P.G. Drazin and W.H. Reid, "*Hydrodynamic Stability,*" (Cambridge University Press, Cambridge, 2nd Ed. 2004), pg. 6